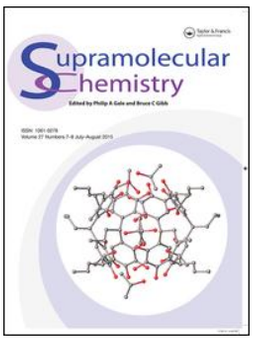

Supramolecular Chemistry

ISSN: 1061-0278 (Print) 1029-0478 (Online) Journal homepage: http://www.tandfonline.com/loi/gsch20

Synergistic catalytic oxidation of cinnamaldehydes by poly(vinyl alcohol) functionalized β-cyclodextrin polymer in CaO_2/HCO_3^- system

Yanxiong Fang, Zujin Yang, Xia Zhang & Hongbing Ji

To cite this article: Yanxiong Fang, Zujin Yang, Xia Zhang & Hongbing Ji (2017): Synergistic catalytic oxidation of cinnamaldehydes by poly(vinyl alcohol) functionalized β-cyclodextrin polymer in CaO_2/HCO_3^- system, Supramolecular Chemistry, DOI: 10.1080/10610278.2017.1371719

To link to this article: http://dx.doi.org/10.1080/10610278.2017.1371719

SUPRAMOLECULAR CHEMISTRY, 2017
https://doi.org/10.1080/10610278.2017.1371719

Taylor & Francis
Taylor & Francis Group

Synergistic catalytic oxidation of cinnamaldehydes by poly(vinyl alcohol) functionalized β-cyclodextrin polymer in CaO_2/HCO_3^- system

Yanxiong Fang[a], Zujin Yang[b,d], Xia Zhang[a] and Hongbing Ji[c,d]

[a]Faculty of Chemical Engineering and Light Industry, Guangdong University of Technology, Guangzhou, China; [b]Fine Chemical Industry Research Institute, School of Chemical Engineering and Technology, Sun Yat-sen University, Guangzhou, China; [c]Fine Chemical Industry Research Institute, School of Chemistry, Sun Yat-sen University, Guangzhou, China; [d]Huizhou Research Institute of Sun Yat-sen University, Huizhou, China

ABSTRACT

Poly (vinyl alcohol) (PVA)–functionalized β-cyclodextrin (β-CD) polymer crosslinked by citric acid (PVA-g-CD) was synthesized, characterized and evaluated for the catalytic oxidation of cinnamaldehydes. The polymer showed good activity and selectivity to aldehydes for some structurally diverse cinnamaldehydes. The enhanced catalytic activity may be attributed to the synergistic effect of the intermolecular weak interactions between β-CD and the functional group of PVA. In addition, calcium peroxide as a solid oxidant was found to significantly affect the reaction. This catalyst can be recovered and reused for five times without a significant loss in its activity and selectivity.

ARTICLE HISTORY
Received 18 June 2017
Accepted 19 August 2017

KEYWORDS
β-CD; poly (vinyl alcohol); catalytic oxidation; natural benzaldehyde; synergistic effect

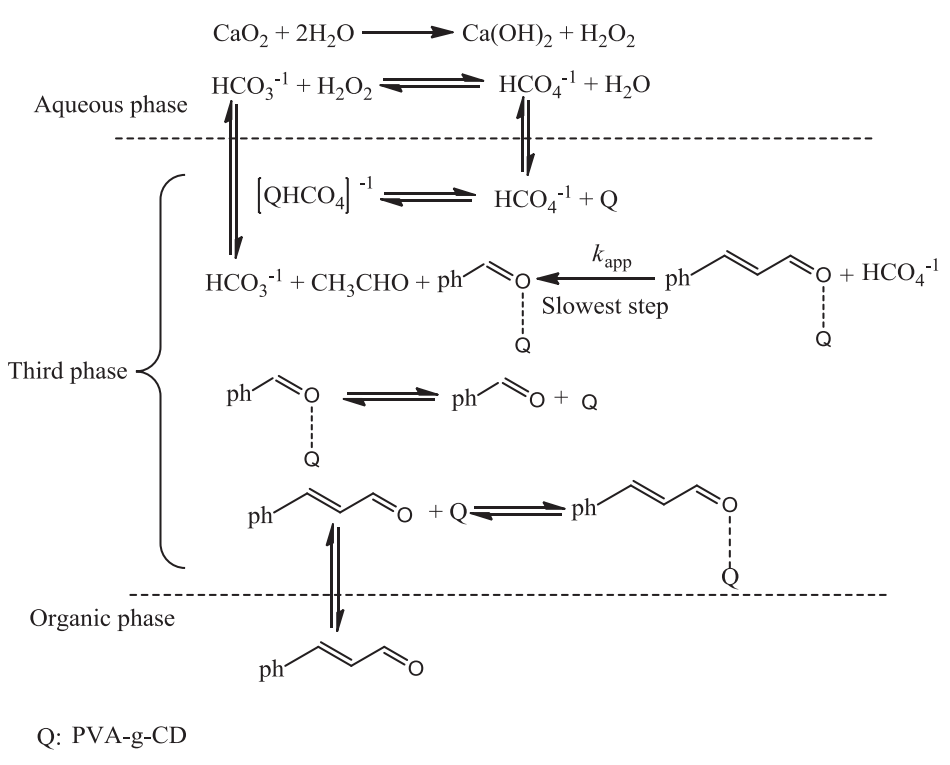

1. Introduction

The market demand of natural benzaldehyde (BzH) as a valuable ingredient for the food, beverages, cosmetics, perfumery, and pharmaceutical industries, is tremendous every year, especially in western countries. The conventional industrial process via the alkaline hydrolysis of laetrile only produces natural BzH that contains toxic hydrogen cyanide (*1*). Therefore, hydrolysis of natural cinnamon oil which contains more than 80% of cinnamaldehyde

CONTACT Zujin Yang Yangzj3@mail.sysu.edu.cn; Hongbing Ji Jihb@mail.sysu.edu.cn
Supplemental data for this article can be accessed at https://doi.org/10.1080/10610278.2017.1371719.

CIN) has attracted considerable attention as an alternative to produce natural BzH (*1–3*). However, the application of these methods has been limited because of the poor solubility of CIN in water and the low selectivity to natural BzH. Phase transfer catalysis (PTC) is a simple and feasible method which has been widely investigated to synthesize some organic chemicals with high yield of products, large reaction rate and high selectivity of the desired products (*4, 5*). In recent years, the liquid phase oxidation of CIN to natural BzH has been carried out with cyclodextrins (CDs) as reverse phase-transfer catalysts (*2, 6–8*).

Cyclodextrins (CDs) are cyclic oligosaccharides with 6–8 D-glucose units linked by *α*-1,4-glucose bonds, which are called α-, β-, and γ-CD, respectively. They have a truncated cone-shaped molecular structure with a relatively hydrophobic inner cavity and hydrophilic outer surface, which can form inclusion complexes with guest molecules in their hydrophobic cavities. By using the specific microenvironment, they can selectively bind substrates in the aqueous phase and catalyze chemical reactions by noncovalent host–guest bonding (*9–14*). Although the catalysts show good catalytic activity for the reaction, the separation of catalysts from the homogeneous system is difficult. Therefore, immobilization of CDs is more appealing because of their many attractive advantages (*15–20*). Firstly, these catalysts can be recovered and reused with good catalytic activity; Secondly, synergistic action between CDs and the functional group of the supports can significantly improve the selectivity of guests. Since β-cyclodextrin (β-CD) is the least expensive among the cyclodextrins, it has been used as the complexing host. Previous studies have reported that water-insoluble β-CD-based polymers (β-CDP) are prepared by the reaction of the hydroxyl groups of CDs with bi- or multi-functional crosslinking agents (*21, 22*). β-CDP, as multi-site phase-transfer catalysts present good catalytic activity with more than one active center and have attracted much attention in the development of phase-transfer catalyzed systems (*17–19*). Epichlorohydrin (EPI) is a common crosslinking reagent for the β-CDP synthesis, but its use has been restricted in the food industry due to its toxicity to human health and the environment (*22, 23*). In comparison to EPI, citric acid has a low toxicity and is friendly to the environment. As a cross-linker, citric acid has been used to synthesize β-CDP at temperatures below 200 °C without any organic solvents or harmful additives (*24*).

Oxidation is an important class of reaction from both industrial and academic points of view. In general, the choice of oxidants is very important for the multiphase reaction system. PTC provides many good opportunities for the oxidation reactions with certain oxidizing agents such as NaOCl, H_2O_2, and $KMnO_4$ (*25, 26*). Among them, H_2O_2 is attractive for the reaction systems, with H_2O as a by-product. However, since H_2O_2 is easily decomposed at high temperature (*27*), the use of the excess amount of H_2O_2 would lead to decrease selectivity of natural BzH (*15, 17–19*). Calcium peroxide (CaO_2) is an environmentally friendly solid oxidizing agent. At a large pH range, CaO_2 can dissolve in water to form H_2O_2 and $Ca(OH)_2$, releasing a maximum of 0.47 g H_2O_2/g CaO_2 (*28–30*). And the release of H_2O_2 can be effectively regulated by the rate of CaO_2 dissolution, thus improving the utilization efficiency of H_2O_2. Therefore, CaO_2 has been widely used for remediation of saturated soil and ground water contaminated by the hazards of gasoline contamination (*28, 31*). However, there has been no study on the application of CaO_2 as an oxidant in preparing natural BzH so far.

In the present work, we synthesized a PVA–functionalized β-CD polymer crosslinked by citric acid (PVA-g-CD, Q) as a new multisite phase-transfer catalyst and CaO_2 as the terminal oxidant for the catalytic oxidation of CIN to natural BzH in aqueous solution. Various physico-chemical techniques were used to characterize the structure of PVA-g-CD. Important factors affecting the reaction rate were investigated systematically and a reasonable mechanism was proposed for the oxidation of CIN.

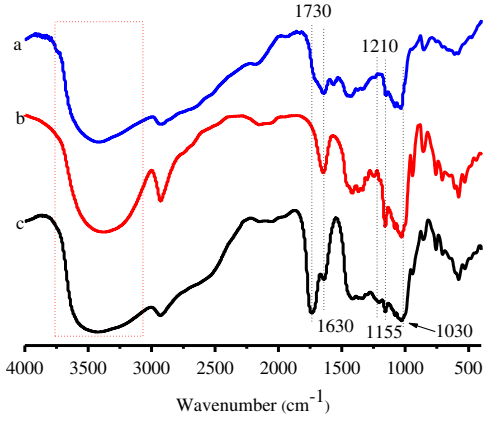

Figure 1. (Colour online) FTIR spectra of PVA (a), β-CD (b), and PVA-g-CD (c).

2. Results and discussion

2.1. Characterization of PVA-g-CD

In order to confirm that PVA was crosslinked with β-CD by using citric acid as crosslinking agent, FTIR spectra of PVA (a), β-CD (b), and PVA-g-CD (c) are shown in Figure 1.

For pure PVA, the characteristic peaks from 2850 to 3000 cm^{-1} are due to C–H broad alkyl stretching band. The broad absorption peak around 3400 cm^{-1} could be assigned to the –OH stretching. The intra- and intermolecular hydrogen bonding also exists among the polymer chains due to high hydrophilic forces. A characteristic

peak at 1140 cm^{-1} is attributed to the crystallization of PVA, which relates to alcoholic C–O stretching vibration (*32*) (Figure 1(a)). From Figure 1(b), the absorption peaks at 3300, 2920, 1646, 1470, and 1030 cm^{-1} correspond to the structure of β-CD (*33*). After preparation of PVA-g-CD, the absorption bands can also be seen in Figure 1(c), implying that the β-CD was grafted on the surface of PVA and the formation of PVA-g-CD well maintained its native structure of β-CD. In addition, an intensive absorption band appears at 1730 cm^{-1} (Figure 1(c)) is assigned to the C=O of carboxyl groups in citric acid. The peak at 1210 cm^{-1} which is attributed to the C–O–C stretching vibration of ester groups is also observed in Figure 1(c). The result indicates that the hydroxyl groups of β-CD have reacted with the carboxyl groups of citric acid and thereby a three-dimensional network can be formed. PVA-g-CD is stable and insoluble because of the cross-linked network. Therefore, FTIR results indicate that the experimental procedure developed in this work is successful in obtaining a water-insoluble β-cyclodextrin grafted poly (vinyl alcohol) cross-linked by citric acid.

The XRD patterns of β-CD (a), PVA (b), and PVA-g-CD (c) are presented in Figure 2. β-CD in its crystalline form displays diffraction peaks at 2θ values of 6.2°, 8.0°, 10.7°, 12.9°, 19.8°, 20.9°, 22.8°, 24.3°, and 36.0° (*33*). PVA has shown a characteristic intense peak at 2θ = 20° corresponding to its crystalline structure (*34*). For the PVA-g-CD, the some characteristic 2θ peaks of β-CD disappeared, and the characteristic peak of PVA at 2θ = 21.3° decreased, shifted, and obviously broadened. The results imply that the chemical modification of PVA with β-CD using citric acid as a cross-linker destroys the original crystallinity of PVA to some extent and β-CD was grafted on the surface of polymer matrix at the molecular level, and no crystals could be observed in the PVA-g-CD.

Figure 3 exhibits the three major weight stages for PVA is in the range of 25–450 °C. For the first stage, mass loss of 7% can be observed from room temperature to 150 °C, which caused by dehydration from PVA. The second stage begins at 200 °C with a major degradation peak at 270 °C with mass loss of 66% due to heat decomposition of PVA. The third stage, which starts at 400 °C, involves the carbonization process of the PVA residue (*35*). PVA-g-CD also shows three weight losses. The first mass loss with the temperature range of 25–160 °C is mainly attributed to the loss of water. The second weight loss observed around 200–310 °C with a major degradation peak at 275 °C is due to the thermal decomposition of PVA in the PVA-g-CD. For the third stage, mass loss could be observed from 310 to 450 °C, which caused by the thermal decomposition of β-CD in the PVA-g-CD (*36*). The second degradation stage of PVA-g-CD exhibits a lower decomposition temperature (180 °C) than that of PVA (220 °C), which demonstrates

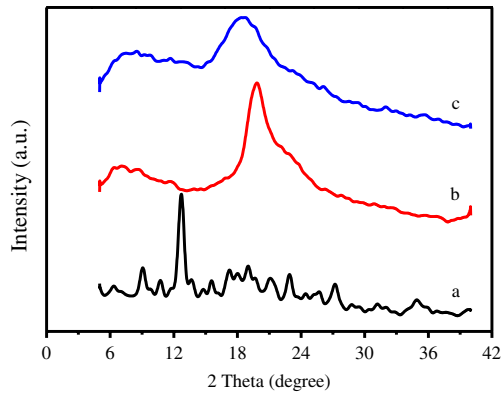

Figure 2. (Colour online) XRD of β-CD (a), PVA (b), and PVA-g-CD (c).

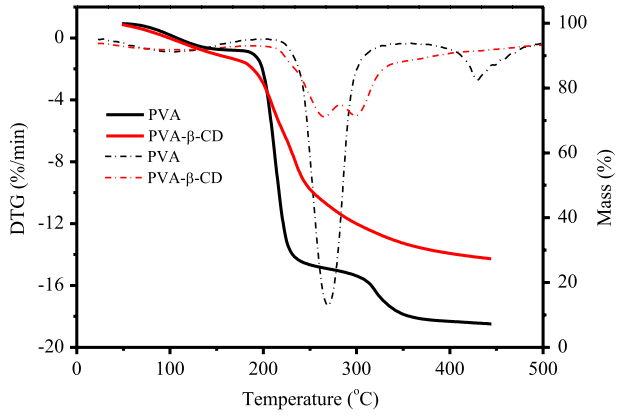

Figure 3. (Colour online) TG and DTG of PVA and PVA-g-CD.

that chemical modification has destroyed intra-molecular hydrogen bonding of PVA, resulting in lower stability.

The ^{13}C NMR can provide some important structural information of the insoluble polymers (*37*). Figure 4 shows the solid-state ^{13}C CP/MAS NMR spectra of PVA (a), β-CD (b), and PVA-g-CD (c).

From Figure 4(a), the signals at about 45 ppm is due to the CH_2 carbon, and the signals at about 65–77 ppm represent the CH carbon. The splitting for the CH carbon is assigned to intra- or intermolecular hydrogen bonding. The signals at 77, 71, and 65 ppm were due to CH with two hydrogen bonds, CH with one hydrogen bond, and CH with no hydrogen bond, respectively. Therefore, the CH peaks have regarded as indicators of the style of intra- or intermolecular molecular hydrogen bonding of -OH groups between two consecutive units of PVA (*38, 39*). The spectrum of β-CD is similar to that previously reported data (*40*) and multiple resonances for each type of carbon atom are shown in Figure 4(b). ^{13}C signals for the glucopyranose unit of β-CD are due to C-1 (103.4 ppm), C-4 (80.6 ppm), C-5 (78.6 ppm), C-3 (74.6 ppm), C-2 (72.4 ppm) and C-6 (59.6 ppm). The spectrum of PVA-g-CD is quite similar to PVA in the solid state, and most of them are observed

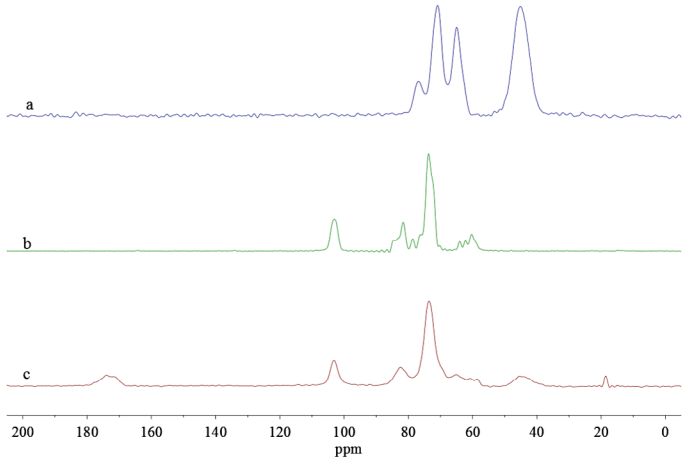

Figure 4. (Colour online) CP/MAS ^{13}C NMR spectra of PVA (a), β-CD (b), and PVA-g-CD (c).

in Figure 4(c), which could be directly assigned to PVA. Moreover, some peaks are observed in the 40–80 ppm region, demonstrating their structure characteristics (*39*). The intensities of the peak, which is assigned to the CH carbon of PVA significantly decreases with addition of β-CD, and a new peak appears at about 175 ppm, which is due to the crosslinking reaction between the OH groups of PVA and the OH groups of β-CD by using citric acid as a crosslinking agent. In addition, the resonances from PVA-g-CD are broad, implying that the crystalline nature of β-CD disappears. The decrease of the C-1signals of β-CD and the increase of the signals in the region between 60 and 70 ppm are due to the hydroxylmethyl group at C-6 in the glucose unit of β-CD. The results clearly show that β-CD was grafted on the surface of PVA by citric acid.

2.2. Catalytic activity investigation

In the present work, the two-phase catalytic oxidation of CIN to natural BzH was successfully synthesized by CaO_2 as the terminal oxidant, PVA-g-CD as the phase-transfer catalyst and $NaHCO_3$ as the cocatalysts, as shown in Scheme 1. The conversion (X) of CIN was defines as:

$$X = 1 - \frac{C_t}{C_o} \tag{1}$$

where C_o is the initial concentration of CIN, C_t is the concentration of CIN at time t, respectively.

The rate expression for this reaction can be calculated from the following equation:

$$-r = k_{app} C_o \tag{2}$$

where k_{app} is the apparent reaction rate constant. This reaction was performed in a reactor, and the reaction rate of CIN with time (t) can be expressed as

$$-\frac{dC_0}{dt} = -r_{CIN} = k_{app} C_o \tag{3}$$

Equation (3) can be transformed to the following function

$$-\ln\left(\frac{C_o}{C_t}\right) = -\ln(1 - X) = k_{app} t \tag{4}$$

k_{app} can be obtained from the slope of linear plot of ln (C_o/C_t) against t.

Under optimized conditions, a high selectivity of product was observed. In the work, no byproducts were detected during the reaction by GC-MS analysis. Only BzH produced from the oxidation of CIN catalyzed by phase-transfer catalysis and cocatalyst in this work. Therefore, the consumption of CIN equaled the yield of BzH. In this section, the effects of the reaction conditions on the conversion of CIN were summarized in the following.

2.2.1. Effect of the cocatalysts

In general, it is difficult to oxidize the organic substance using the water-soluble oxidant agent. Therefore, it is necessary to investigate the role of these oxidant agents, phase-transfer catalysts, or cocatalysts to promote the reaction. In this work, $NaHCO_3$ was used as the cocatalyst. As shown in Figure 5, 60% conversion of CIN was observed in the presence of CaO_2, PVA-g-CD, and $NaHCO_3$ in aqueous solutions. The conversion was significantly decreased at the absence of any one of the components. In the reaction, QCIN was synthesized, and then CaO_2 would dissolve in water to liberate H_2O_2, and the active oxidant-peroxymonocarbonate ion (HCO_4^{-1}), with structure $HOOCO_2^{-1}$ formed by a reaction between bicarbonate ion and H_2O_2 in the aqueous solutions. Finally, the true oxidant agent HCO_4^{-1} was then transferred to the third phase by the

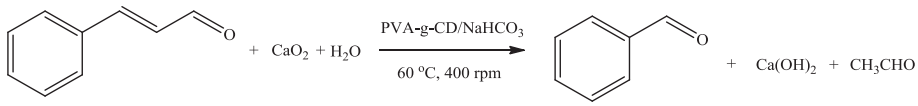

Scheme 1. (Colour online) Oxidation of cinnamaldehyde with PVA-g-CD as phase-transfer catalyst and CaO_2 as the terminal oxidant.

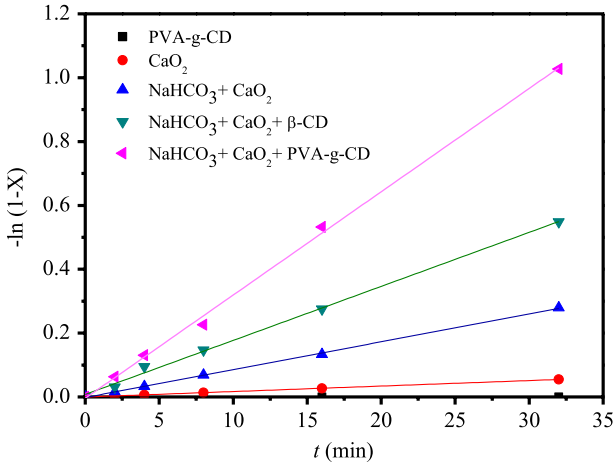

Figure 5. (Colour online) Effects of the oxidant agent, cocatalyst, and phase transfer catalyst on the conversion of cinnamadehyde: cinnamadehyde (1 mmol), PVA-g-CD (0.8 g), CaO_2 (1 mmol), $NaHCO_3$ (2 mmol), 400 rpm, 60 °C, 32 min.

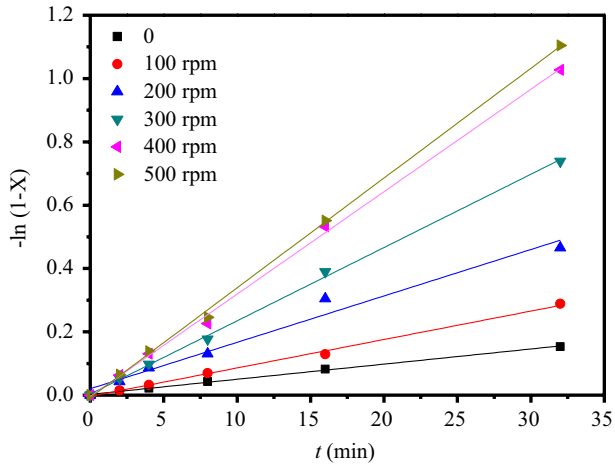

Figure 6. (Colour online) Effects of stirring speed on the conversion of cinnamadehyde: cinnamadehyde (1 mmol), PVA-g-CD (0.8 g), CaO_2 (1 mmol), $NaHCO_3$ (2 mmol), 60 °C, 32 min.

phase-transfer catalyst (Q) for further reaction with CIN. As a phase-transfer catalyst, PVA-g-CD showed much better catalytic activity than that of β-CD, implying the synergistic effects via the various intermolecular weak interactions between β-CD and the functional group of PVA. The effect of the different components on the apparent rate constant, k_{app}, was shown in Table 1.

2.2.2. The effect of agitation speed

For a liquid–solid–liquid three-phase reaction system, the conversion of the three-phase reaction is significantly affected by the mass transfer. The effect of agitation speed on the conversion of CIN was investigated in the range of 0–500 rpm in the presence of phase transfer catalyst, PVA-g-CD, as shown in Figure 6.

As shown in Figure 6, the conversion of CIN increased with increasing agitation speed from 100 to 500 rpm. However, the increase of CIN conversion was negligible beyond an agitation speed of 400 rpm. As solid PTC was added in the aqueous solution, the complex of QCIN was influenced by the speed of agitation due to enhancement of mass transfer. With the increase in the number of QCIN complex, subsequent oxidation of CIN to natural BzH was observed. The experimental data for the reaction kinetics obeyed the pseudo-first-order rate law and passed the point of origin a straight line for each experimental run. k_{app} were obtained from the slope of the straight lines. A plot of k_{app} and various agitation speeds were shown in Table 2. The apparent rate constant increased linearly when the agitation speed was increased. The mass transfer rate almost reached a constant value when the agitation speed was above 400 rpm. Therefore, the agitation speed was set at 400 rpm for further experiments.

Table 1. Apparent rate constants under different catalytic systems.

Components	PVA-g-CD	CaO_2	CaO_2 + $NaHCO_3$	$NaHCO_3$ + CaO_2 + β-CD	CaO_2 + $NaHCO_3$ + PVA-g-CD
$K_{app} \times 10^2$ (min^{-1})	0	0.172	0.873	1.692	3.234

2.2.3. The effect of PVA-g-CD amount

In general, the reactivity was increased with increasing in the amount of PVA-g-CD. In the work, PVA-g-CD as phase-transfer catalysts was added to the reaction mixture for enhancing the transfer rate of CIN. Thus, the amount of PVA-g-CD would affect the reaction rate of CIN, and the results were shown in Figure 7.

As shown in Figure 7, the conversion of CIN was increased with increasing the amount of PVA-g-CD. The rate constants were linearly dependent on the amount of catalyst from 0 g to 0.8 g in the reaction. A further increase in the amount of PVA-g-CD did not increase the reaction rate significantly. It was attributed that more number of PVA-g-CD molecules provided more number of QCIN

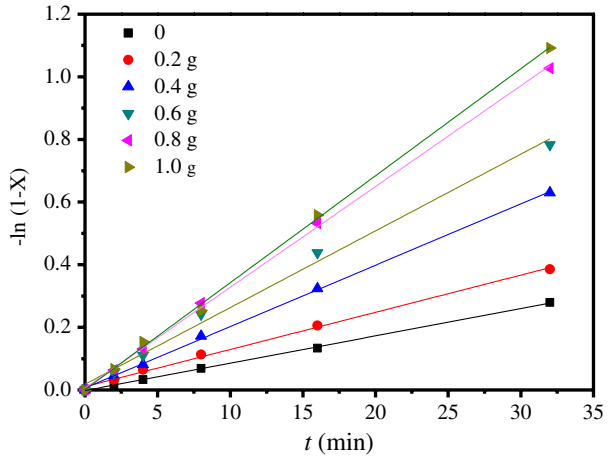

Figure 7. (Colour online) Effects of the amount of PVA-g-CD on the conversion of cinnamadehyde: cinnamadehyde (1 mmol), CaO_2 (1 mmol), $NaHCO_3$ (2 mmol), 400 rpm, 60 °C, 32 min.

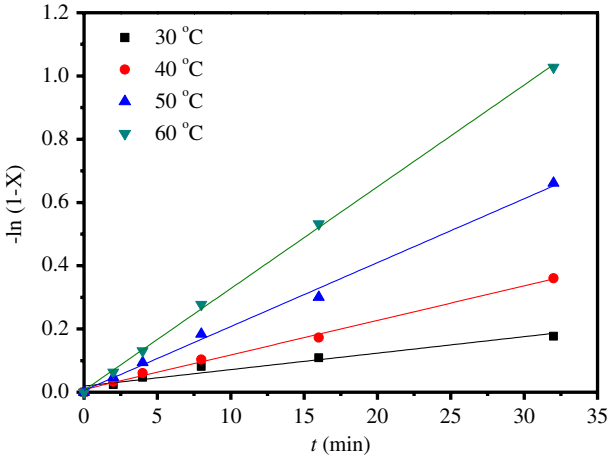

Figure 8. (Colour online) Effects of reaction temperature on the conversion of cinnamadehyde: cinnamadehyde (1 mmol), CaO_2 (1 mmol), PVA-g-CD (0.8 g), $NaHCO_3$ (2 mmol), 400 rpm, 32 min.

Table 2. Apparent rate constants under various agitation speeds.

Agitation speed (rpm)	0	100	200	300	400	500
$K_{app} \times 10^2$ (min^{-1})	0.478	0.898	1.465	2.314	3.234	3.467

Table 3. The rate orders and rate constants at different reaction temperatures in the presence and absence of PVA-g-CD.

Temperature (°C)	In the presence of PVA-g-CD			In the absence of PVA-g-CD		
	n	k (min^{-1})	R	n	k (min^{-1})	R
30	1	0.00521	0.9948	1	0.0001024	0.9978
40	1	0.01092	0.9956	1	0.0004048	0.9951
50	1	0.0238	0.9947	1	0.0008187	0.9987
40	1	0.03218	0.9991	1	0.0016296	0.9914

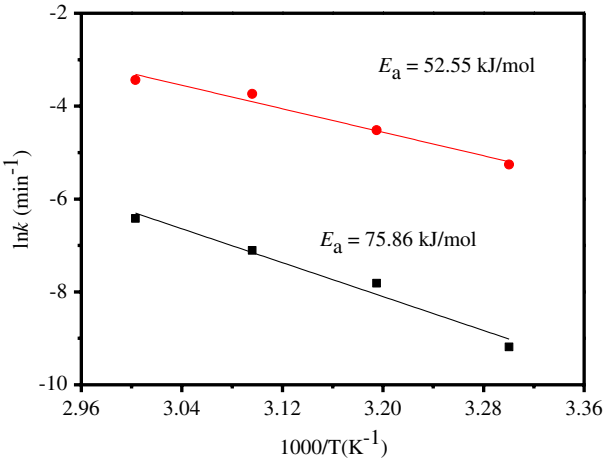

Figure 9. (Colour online) Arrhenius plot: dependence of k_{app} on temperature.

Table 4. Effects of amount of CaO_2 on the conversion of cinnamadehyde.[a]

Entry	CaO_2	Conversion (%)	Selectivity (%)
1	0	5.4	74.4
2	0.25	36.9	83.6
3	0.5	48.8	91.9
4	1	60.0	100
5	1.25	72.5	92.4

[a]Reaction conditions: cinnamadehyde (1 mmol), PVA-g-CD (0.8 g), $NaHCO_3$ (2 mmol), 400 rpm, 32 min.

complex which resulted in the formation of CIN available for the oxidation reaction. However, the further increase inevitably led to the decrease of BzH selectivity. It was due to the excess oxidation of BzH to benzoic acid. Therefore, the conversion was obviously affected by the amount of PVA-g-CD, so 0.8 g of PVA-g-CD per 25 ml water was used for the study.

2.2.4. The effect of temperature

Effect of reaction temperature on the oxidation of CIN was studied in the temperature range of 30–60 °C as shown in Figure 8.

As Figure 8 showed the conversion of CIN increased with increasing the reaction temperature and the product yields in 32 min of reaction were 16.2% for 30 °C, 30.3% for 40 °C, 48.4% for 50 °C, and 60.2% for 60 °C, respectively. The apparent rate constant increased with the increasing temperature from 30 °C to 60 °C and could well follow the pseudo-first-order kinetic model in the presence and absence of PVA-g-CD (Table 3). By applying Arrhenius' equation, plots of ln k and 1/T were drawn in Figure 9. The plots were of good linearity and the activation energies E_a in the presence and absence of PVA-g-CD were calculated to be 75.86 and 52.55 kJ mol^{-1}, respectively. It is obvious that the oxidation of CIN was promoted by the PVA-g-CD,

Table 5. Effects of amount of $NaHCO_3$ on the conversion of cinnamadehyde.[a]

Entry	$NaHCO_3$ (mmol)	Conversion (%)	Selectivity (%)
1	0	4.0	65.1
2	0.5	4.7	68.1
3	1	5	68.0
4	1.25	40	79.9
5	1.5	52.5	89.9
6	2	60	100
7	2.25	70.8	90.9

[a]Reaction conditions: cinnamadehyde (1 mmol), CaO_2 (1 mmol), PVA-g-CD (0.8 g), 400 rpm, 32 min.

implying that the PVA-g-CD indeed contributed to the considerable improvement of activity, thus PVA-g-CD was an efficient phase transfer catalyst for the oxidation of CIN.

2.2.5. The effect of amount of CaO_2

As shown in Table 4, the amount of CaO_2, which dissolved to form H_2O_2 had a significant influence on the oxidation of CIN. The conversions of CIN and selectivity to BzH were 5.4% and 74.4% with the absence of CaO_2 at 60 °C and a reaction time of 32 min, and they were increase to 60% and 100%, respectively, when 1 mmol of CaO_2 was present. However, further increase the amount of CaO_2 to 1.25 mmol leaded to selectivity of BzH decrease to 92.4%. According to stoichiometry, the molar ratio between H_2O_2 and CIN is 1:1. In the work, the molar ratio of CaO_2 and CIN is 1:1, which was significantly lower that of H_2O_2 used in the reaction (22:1) (*17, 20*). Therefore, 1 mmol CaO_2 was regarded as the appropriate amount under the conditions employed in this work.

2.2.6. The effect of amount of $NaHCO_3$

Hydrogen peroxide is an oxygen-rich, environmentally friendly oxidant, but it is a rather slow oxidizing agent in the absence of activators. Richardson et al. (*41, 42*) described bicarbonate anion is an efficient activator for hydrogen peroxide to generate peroxymonocarbonate (HCO_4^-), which could effectively oxidize CIN to produce BzH (*17, 18*).

As shown in Table 5, in the absence of $NaHCO_3$, the conversion of CIN and the selectivity of BzH were only 4.0% and 65.1%, respectively. Increasing the amount of $NaHCO_3$ to 1 mmol, the same results were observed due to the formation of calcium carbonate by the reaction of sodium hydrogen carbonate and sodium carbonate. When the amount of $NaHCO_3$ was from 1 mmol to 2 mmol, CIN conversion and BzH selectivity were increased to 60% and 100%, respectively, which indicated that $NaHCO_3$ played a crucial role in the oxidation of CIN. Further increasing the amount of $NaHCO_3$ to 2.25 mmol increased the CIN conversion to 70.8%, while decreased the selectivity to BzH to 90.9% due to the excess oxidation of BzH to benzoic acid.

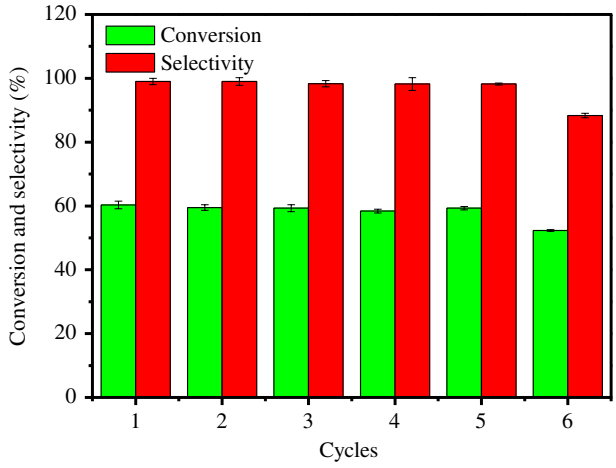

Figure 10. (Colour online) Reusability of the catalyst. Reaction conditions: cinnamadehyde (1 mmol), PVA-g-CD (0.8 g), CaO_2 (1 mmol), $NaHCO_3$ (2 mmol), 400 rpm, 32 min.

Therefore, an appropriate amount of $NaHCO_3$ is necessary for the reaction (2 mmol).

2.3. The oxidation of substituted cinnmaldehydes

As shown in Table 6, we further optimized and investigated the oxidation of substituted cinnamaldehydes to the corresponding benzaldehydes. As shown in Table 6, the oxidation of substituted cinnamaldehydes to the corresponding benzaldehydes was performed smoothly in good conversion and excellent selectivity. However, the electronic natures of substituent groups on the cinnamaldehydes have some impact on their catalytic oxidation. The oxygen-containing groups (entries 1–3, 10–12) substituted cinnamaldehydes produce the corresponding benzaldehydes in 95–99% selectivity with reaction rates of 0.0212 to 0.0252 min^{-1}, which were much higher than those of the cinnamaldehydes. It was attributed that they were able to form the inclusion complexes by hydrogen bonds of the $-OCH_3$ or $-NO_2$ groups to secondary hydroxyl groups on the rim of the β-CD, which could improve the selectivity and reaction rate of substances. In addition, the steric hindrance of the substituent groups also significantly affected their catalytic activity. Conversion, selectivity, and reaction rate of the o- (entries 1, 4, 7, and 10), m- (entries 2, 5, 8 and 11) and p-(entries 3, 6, 9 and 12) substituted cinnamaldehydes presented an increased tendency. The electron-rich methoxyl- (entries 1–3) and electron-neutral methyl-(entries 4–6) substituted cinnamaldehydes could give the corresponding benzaldehydes in 55–60% conversion and 95–99% selectivity, respectively. While for the electron-withdrawing chloride- and nitro-substituted substituted cinnamaldehydes, the conversion and selectivity can only achieve in 50–55% and 90–99% (entries 6–12), respectively. The

results in Table 6 clearly showed that the weak interactions between β-CD and substrates could enhance their reaction activity, which depended on the size, shape and hydrophobicity of the guest molecules.

Table 6. Oxidation of substituted cinnamaldehydes to the corresponding aldehydes over PVA-g-CD and CaO_2 in water.[a]

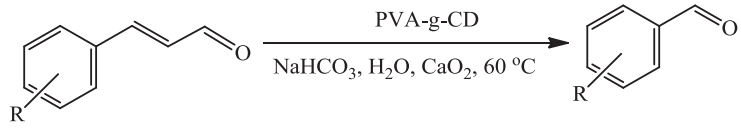

Entry	Reactant	Product	k_{app} (min^{-1})	Conversion (%)	Selectivity (%)
1	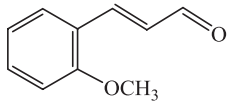	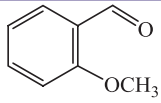	0.0212	57	96
2	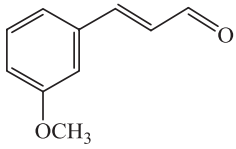	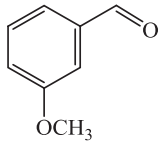	0.0236	58	98
3	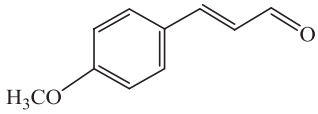	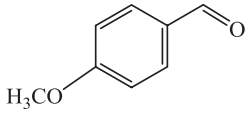	0.0241	60	99
4	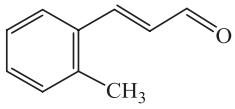	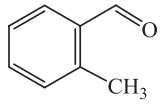	0.0162	54	95
5	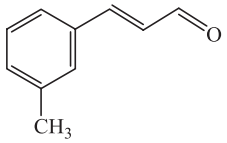	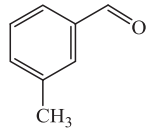	0.0178	57	97
6	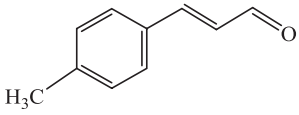	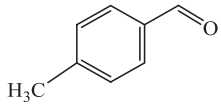	0.0189	60	99
7	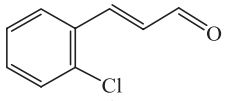	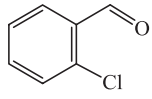	0.0149	50	90
8	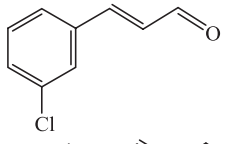	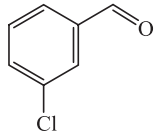	0.0155	53	92
9	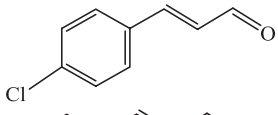	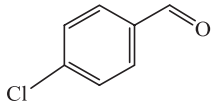	0.0162	54	95
10	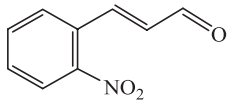	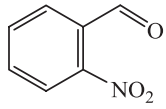	0.0228	52	96
11	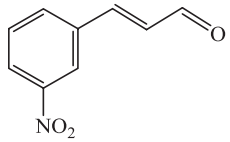	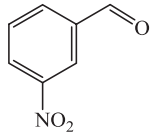	0.0231	54	98
12	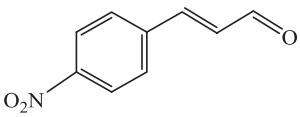	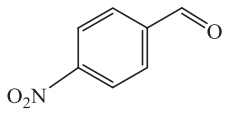	0.0252	55	99

[a]Reaction conditions: cinnamadehyde (1 mmol), PVA-g-CD (0.8 g), CaO_2 (1 mmol), $NaHCO_3$ (2 mmol), 400 rpm, 32 min.

2.4. Reusability of the catalyst

In order to assess the stability of the catalyst, the catalyst was filtered by centrifugation at 3,000 rpm from the reaction mixture, washed with ethanol and water at 60 °C for 2 h, respectively. After dried, the catalyst was reused for the next run under the same conditions. As shown in Figure 10, the catalyst could be reused at least five times with similar conversions of CIN and selectivity for natural BzH, which indicated that the synthesized PVA-g-CD is a stable catalyst. After reaction, the β-CD content of used catalyst was analyzed with phenolphthalein (*43*), and the result indicated that the β-CD content changed from 13.5% to 13.0%, which showed that the structure of these catalysts did not changed in the catalytic oxidation. Compared with the very recently reported catalysts, as shown in Table 7, the present results exhibit significant advantages in terms of the selectivity of BzH. Therefore, the study may be helpful for designing the more efficient catalysts and oxidizers, which can be conveniently prepared and applied in large scale.

Table 7. Performance comparison among various β-CD based catalysts for the oxidation of cinnamaldehyde to benzaldehyde.

Catalysis	Selectivity (%)	Refs
PVA-g-CD	100	This work
2-HP-β-CDCP	84	15
β-CDCP	71	16
β-CDP	62	17
β-CD-CTS	78	19
MWCNTs-g-CD	85	20

2.5. Mechanism

The reaction between CIN and CaO_2 in water using PVA-g-CD as phase transfer catalyst obeyed a solid-liquid-liquid phase transfer mechanism (Scheme 2). Firstly, CIN would be adsorbed onto the surface of PVA-g-CD through weak hydrogen bonding under mechanical stirring. Based on the lower binding energy (Table s1), β-CD site on the surface of PVA-g-CD captured CIN into its cage structure and formed a more stable inclusion complex at the interface between third phase and organic phase. The results are in good agreement with the previously reported data (*15–18, 20, 40*). Secondly, with vigorously stirring, a known amount of CaO_2 was added slowly into the mixture, and then they can carry out a complete reaction to release H_2O_2. With the addition of $NaHCO_3$, an active oxidant peroxymonocarbonate ion, HCO_4^{-1}, with structure of $HOOCO_2^{-1}$ formed by activating hydrogen peroxide with bicarbonate ion. HCO_4^{-1} was adsorbed onto the PVA-g-CD surfaces, went into the third phase. The generated HCO_4^{-1} could react with CIN to yield its epoxide. In situ generated HCO_4^{-1} can subsequently react with the as-prepared epoxide to produce the BzH. Finally, the catalyst restores its initial state. The data suggests a solid-liquid-liquid phase transfer mechanism in accordance with previously published studies (*15, 20*).

3. Conclusions

In conclusion, an efficient and eco-friendly process for the oxidation of CIN to natural BzH over PVA-g-CD catalyst

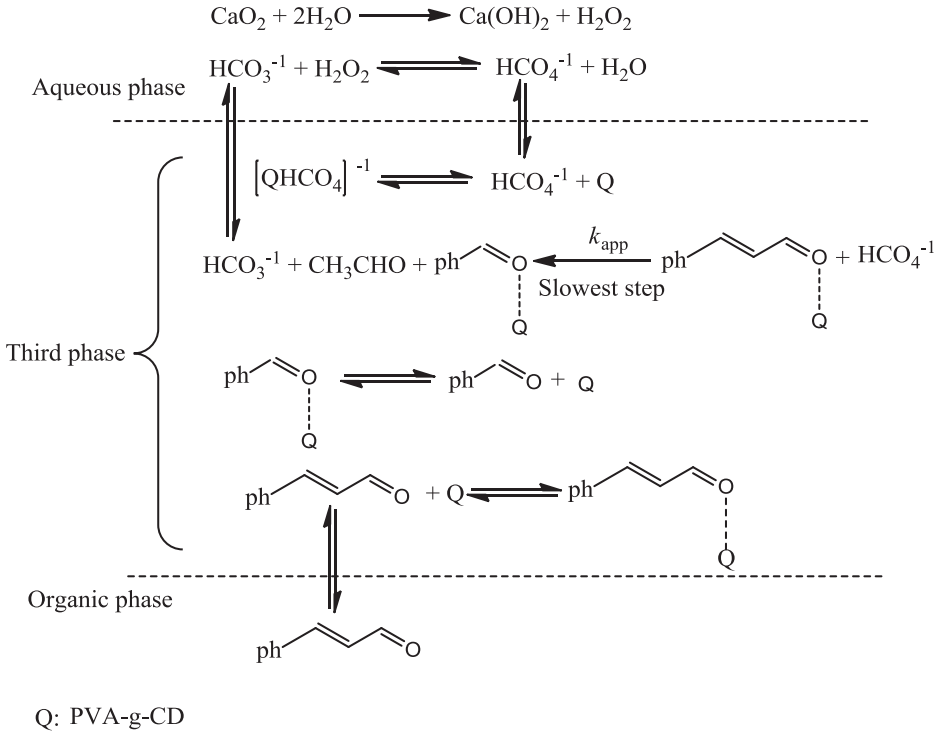

Scheme 2. (Colour online) Oxidation of cinnamaldehyde to benzaldehyde.

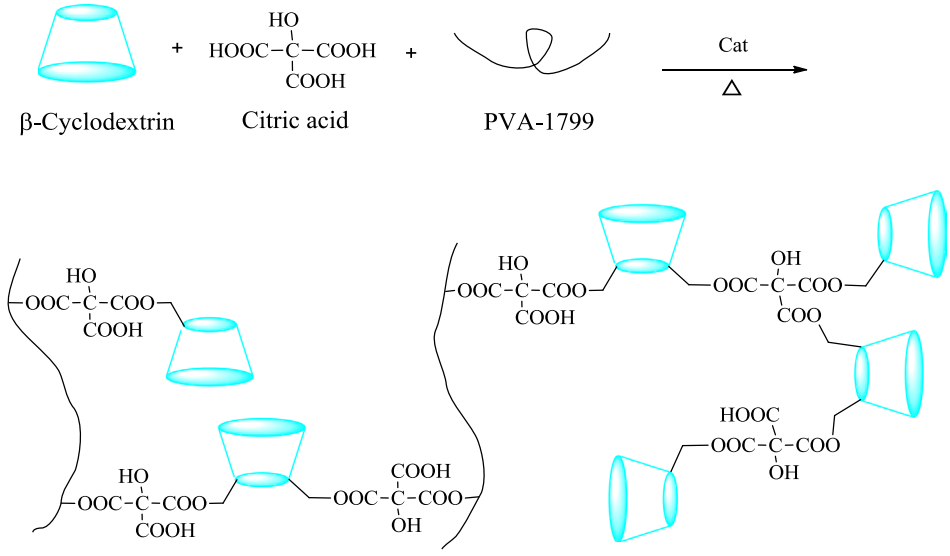

Scheme 3. (Colour online) Synthetic procedure and possible chemical structures of PVA-g-CD.

combined with CaO_2 as the terminal oxidant was studied in this work. The factors affecting the reaction rate of CIN, such as agitation speed, amount of PVA-g-CD, temperature, amount of CaO_2, and amount of $NaHCO_3$ were investigated to determine the optimal operating conditions. Under the optimized conditions, 60% conversion of CIN with 100% selectivity to natural BzH was obtained with a short reaction time of 32 min. The reaction was not affected by agitation speed higher than 400 rpm. The reaction rate increased with increasing temperature, catalyst amount, cocatalyst amount and oxidant amount and obeyed the pseudo-first order kinetics. The catalyst was recyclable for up to five runs consecutively without any appreciable loss of activity and selectivity. Since the PVA-g-CD catalyst is able to oxidize CIN to natural BzH with high selectivity, highly recyclable, remarkably stable and above all, environmentally friendly, they hereby are promising for the industrial application.

4. Experimental section

4.1. General

PVA-1799 (hydrolysis degree ≥ 99%; DP = 1799) was supplied from Sichuan Vinylon Factory, China. Cinnamaldehyde (> 99%) was obtained from Sinopharmacy Chemical Reagent, China. β-CD (> 99%) was purchased from Shanghai Boao Biotechnology, China. CaO_2 was synthesized and characterized in the supplementary material (Figures S1–S3). All other chemicals were purchased in analytical purity and used without further purification and all solutions were prepared with distilled water under ambient conditions.

4.2. Preparation of PVA-g-CD

PVA-g-CD was synthesized according to the previous Refs. with minor modification (*44, 45*). The detail synthesis of PVA-g-CD was as following: a mixture of β-CD (2 g), citric acid monohydrate (1 g), sodium dihydrogen phosphate (0.1 g), PVA-1799 (0.2 g), and deionized water (10 mL) was stirred to homogeneous at 40 °C in a water bath for 2 h. It was heated to 140 °C in an electric thermostatic oven and kept the same temperature for 4 h. After the reaction, the reaction mixture was cooled to room temperature, and the solids were purified by soaking, washed to neutral pH, and dried under vacuum at 60 °C to obtain PVA-g-CD, as showed in Scheme 3. β-CD content of PVA-g-CD was calculated as 0.119 mmol/g according to the previously reported method (*43*).

4.3. Characterization techniques

Fourier transform infrared (FTIR) spectra of β-CD, PVA, and PVA-g-CD were recorded on a Bruker TENSOR 37 FTIR spectrometer as KBr pellets in the 4000–400 cm^{-1} spectral range. TG-DTG curves were obtained on a Netzsch STA-449C thermal analysis system. The samples were put inside the platinum pans, which were hanging in the heating furnace. The weight percentage of the residue was recorded while the furnace was heating from 25 to 450 °C. The flow rate of nitrogen was about 40 mL/min, and a heating rate of 10 °C/min was employed. X-ray diffraction (XRD) was carried out on D/max-2200/PC X-ray Diffractometer with an area detector using a Cu *K*α radiation source (λ = 1.54056 Å) to study the crystal structure of the CaO_2.

X-ray photoelectron spectroscopy (XPS, ESCALab250) was used to analyze the elemental sates. Transmission electron microscopy (TEM, JEOL S-520) was used to examine the surface morphology and the particle size of the solid oxidant. The solid-state CP/MAS ^{13}C NMR data of β-CD, PVA, and PVA-g-CD were performed on Bruker Avance II 500 MHz spectrometer to determine the successful graft of β-CD on the surface of PVA.

4.4. Oxidation of CIN

CIN (1 mmol), PVA-g-CD (0.8 g), and water (25 mL) were added into a 50 mL three-necked flask fitted with a reflux condenser and magnetic stirrer. The mixture was heated to 60 °C in an oil bath with electric heater, and then CaO_2 (1 mmol) and $NaHCO_3$ (2 mmol) were slowly added into the mixture. The resulting system was stirred with magnetic stirrer at 60 °C for 32 min. At the end of the reaction, the resulting products and unreacted CIN were extracted twice with 25 mL ethyl acetate. Samples were taken at appropriate intervals and extracted by ethyl acetate and then centrifuged. The supernatants were analyzed and identified by gas chromatography mass spectrometer (GC-MS) including an Agilent HP5977A mass spectrometer attached to an Agilent 7890B gas chromatograph with a HP-5 column. The reproducibility for all the data was within 5%.

Disclosure statement

No potential conflict of interest was reported by the authors.

Funding

This work was preliminarily supported by the National Natural Science Foundation of China [grant number 21376279], [grant number 21425627]; the National Natural Science Foundation of China-SINOPEC Joint fund [grant number U1663220]; the Natural Science Foundation of Guangdong Province [grant number 2017A030313057]; the China and Guangdong Technology Research Center for Synthesis and Separation of Thermosensitive Chemicals [grant number 2015B090903061].

ORCID

Zujin Yang http://orcid.org/0000-0003-2319-3055

References

(1) Chen, H.Y.; Ji, H.B. *AIChE J.* **2010**, *56*, 466–476.
(2) Chen, H.Y.; Ji, H.B.; Zhou, X.T.; Wang, L.F. *Tetrahedron.* **2010**, *66*, 9888–9893.
(3) Chen, H.Y.; Ji, H.B.; Zhou, X.T. *Catal. Commun.* **2009**, *10*, 828–832.
(4) Naik, S.D.; Doraiswamy, L.K. *AIChE J.* **1988**, *44*, 612–646.
(5) Chief Elk, J.; Benjamin, I. *Langmuir.* **2015**, *31*, 5086–5092.
(6) Chen, H.Y.; Yang, Z.J.; Zhou, X.T.; Ji, H.B. *Supramol. Chem.* **2012**, *24*, 247–254.
(7) Nie, Y.M.; An, Y.P.; Peng, C.H.; Yao, X.D. *Appl. Mech. Mate.* **2014**, *522–524*, 458–464.
(8) Chen, H.Y.; Ji, H.B. *Chinese. J. Chem. Eng.* **2011**, *19*, 972–977.
(9) Takahashi, K. *Chem. Rev.* **1998**, *98*, 2013–2034.
(10) Surendra, K.; Krishnaveni, N.S.; Reddy, M.A.; Nageswar, Y.V.D.; Rao, K.R. *J. Org. Chem.* **2003**, *68*, 2058–2059.
(11) Luo, J.; Yu, H.; Wang, H.J.; Wang, H.H.; Peng, F. *Chem. Eng. J.* **2014**, *240*, 434–442.
(12) Luo, J.; Peng, F.; Yu, H.; Wang, H.H.; Zheng, W. *ChemCatChem.* **2013**, *5*, 1578–1586.
(13) Kumar, A.; Tripathi, V.D.; Kumar, P. *Green. Chem.* **2011**, *13*, 51–54.
(14) Krishnaveni, N.S.; Surendra, K.; Rama Rao, K.. *Adv. Synth. Catal.* **2004**, *346*, 346–350.
(15) Yang, Z.J.; Ji, H.B. *ACS Sustain. Chem. Eng.* **2013**, *1*, 1172–1179.
(16) Yang, Z.J.; Ji, H.B. *Chinese J. Catal.* **2014**, *35*, 590–598.
(17) Yang, Z.J.; Zeng, H.; Zhou, X.T.; Ji, H.B. *Tetrahedron* **2012**, *68*, 5912–5919.
(18) Yang, Z.J.; Jiang, H.G.; Zhou, X.T.; Fang, Y.X.; Ji, H.B. *Supramol. Chem.* **2012**, *24*, 379–384.
(19) Yang, Z.J.; Zeng, H.; Zhou, X.T.; Ji, H.B. *Supramol. Chem.* **2013**, *25*, 233–245.
(20) Yang, Z.J.; Zhang, X.; Fang, Y.X.; Rui, Z.; Ji, H.B. *Chinese J. Catal.* **2016**, *37*, 2086–2097.
(21) Ozmen, E.Y.; Sezgin, M.; Yilmaz, A.; Yilmaz, M. *Bioresource. Technol.* **2008**, *99*, 526–531.
(22) Morin-Crini, N.; Crini, G. *Prog. Polym. Sci.* **2013**, *38*, 344–368.
(23) Crini, G. *Prog. Polym. Sci.* **2005**, *30*, 38–70.
(24) Zhao, D.; Zhao, L.; Zhu, C.S.; Tian, Z.B.; Shen, X.Y. *Carbohyd. Polym.* **2009**, *78*, 125–130.
(25) Jose, N.; Sengupta, S.; Basu, J.K. *J. Mol. Catal. A- Chem.* **2009**, *309*, 153–158.
(26) Satrio, J.A.B.; Doraiswamy, L.K. *Chem. Eng. J.* **2001**, *82*, 43–56.
(27) Ishihara, T.; Ohura, Y.; Yoshida, S.; Hata, Y.; Nishiguchi, H.; Takita, Y. *Appl. Catal.A: Gen.* **2005**, *291*, 215–221.
(28) Northup, A.; Cassidy, D. *J. Hazard. Mater.* **2008**, *152*, 1164–1170.
(29) Qian, Y.; Zhou, X.; Zhang, Y.; Sun, P.; Zhang, W.; Chen, J.; Guo, X.; Zhang, X. *Chem. Eng. J.* **2015**, *279*, 538–546.
(30) Ma, J.; Song, W.; Chen, C.; Ma, W.; Zhao, J.; Tang, Y. *Environ. Sci. Technol.* **2005**, *39*, 5810–5815.
(31) Zhang, X.; Gu, X.; Lu, S.; Miao, Z.; Xu, M.; Fu, X.; Qiu, Z.; Sui, Q. *J. Hazard. Mater.* **2015**, *284*, 253–260.
(32) Mansur, H.S.; Oréfice, R.L.; Mansur, A.A.P. *Polymer.* **2004**, *45*, 7193–7202.
(33) Yang, Z.J.; Xiao, Z.B.; Ji, H.B. *Flavour. Frag. J.* **2015**, *30*, 179–187.
(34) Lu, J.; Wang, T.; Drzal, L.T. *Compos. Part A- Appl. S.* **2008**, *39*, 738–746.
(35) Chiellini, E.; Cinelli, P.; Fernandes, E.G.; Kenawy, E.R.S.; Lazzeri, A. *Biomacromolecules.* **2001**, *2*, 806–811.
(36) Yang, Z.J.; Huang, L.; Yao, X.D.; Ji, H.B. *Flavour. Frag. J.* **2017**, *32*, 102–111.
(37) Crini, G.; Cosentino, C.; Bertini, S.; Naggi, A.; Torri, G.; Vecchi, C.; Janus, L.; Morcellet, M. *Carbohyd. Res.* **1998**, *308*, 37–45.
(38) Kobayashi, M.; Ando, I.; Ishii, T.; Amiya, S. *Macromolecules* **1995**, *28*, 6677–6679.
(39) Miyoshi, T.; Takegoshi, K.; Hikichi, K. *Polymer* **1997**, *38*, 2315–2320.

(40) Yang, Z.J.; Zhang, X.; Yao, X.D.; Fang, Y.X.; Chen, H.Y.; Ji, H.B. *Tetrahedron* **2016**, *72*, 1773–1781.
(41) Yao, H.; Richardson, D.E. *J. Am. Chem. Soc.* **2003**, *125*, 6211–6221.
(42) Yao, H.; Richardson, D.E. *J. Am. Chem. Soc.* **2000**, *122*, 3220–3221.
(43) Basappa, C.; Rao, P.; Rao, D.N.; Divakar, S. *Int. J. Food. Sci. Tech.* **1998**, *33*, 517–520.
(44) Zhao, D.; Zhao, L.; Zhu, C.S.; Shen, X.; Zhang, X.; Sha, B. *J. Hazard. Mater.* **2009**, *171*, 241–246.
(45) Zhao, D.; Zhao, L.; Zhu, C.S.; Huang, W.Q.; Hu, J.L. *J. Incl. Phenom. Macro. Chem.* **2009**, *63*, 195–201.